Interpretation of Uptake Coefficient Data Obtained with Flow Tubes

E. James Davis

Department of Chemical Engineering, University of Washington, Box 351750, Seattle, Washington 98195-1750

Received: June 25, 2007; In Final Form: December 19, 2007

The uptake of trace gases such as OH and HO_2 radicals, NH_3, $ClONO_2$, N_2O_5, ozone, and many other gases by water, aqueous solutions of acids, and salts has been reported by numerous investigators using a variety of techniques. Reported uptake coefficients vary greatly, ranging from 10^{-8} to 1. This paper describes a new analysis of uptake data obtained in flow tubes that consolidates data obtained for various flow rates and trace gas concentrations. Previous analyses, which have been often used, are shown to be limiting cases or special cases of the analysis outlined here. Of particular emphasis are results for wetted-wall columns and trace gas uptake by aerosol entrained in flow tubes. In the absence of aerosol, the analysis is shown to predict the decrease in trace gas concentration due to bulk chemical reaction and/or reaction at the tube wall or gas−liquid interface. Uptake coefficients for OH and HO_2 radicals on water in wetted-wall tubes are shown to range from 0.01 to 1, and on sulfuric acid, they vary from 0.008 to 0.03. For O_3 on a water film doped with a scavenger, the uptake coefficient is found to be 0.0008. Uptake coefficients determined by different techniques are compared.

Introduction

Heterogeneous gas−liquid reactions have a significant impact on atmospheric chemistry involving processes such as the production of acid rain, ozone depletion, and haze and smog formation. Because of this influence, numerous studies of the uptake of trace gases by water droplets, aqueous solutions of H_2SO_4, and other aerosols have been reported in the last two decades, as evidenced by the extensive reviews of Kolb et al.[1] and Davidovits et al.[2] Several experimental methods have been used to measure uptake coefficients of trace gases such as OH[3−5] and HO_2[3,5−7] radicals, $ClONO_2$,[8−11] HCl,[8,12,13] HOCl,[12] NH_3,[14] N_2O_5,[9,11,15−18] O_3,[18,19] SO_2,[20] and others. The most frequently used technique is the droplet train method in which a stream of droplets pass through a vertical flow tube maintained at sub-atmospheric pressure. The concentration of the trace gas in the gas phase is usually monitored by mass spectrometry or other methods to determine the uptake. Flow tubes in which a polydisperse aerosol is entrained in a carrier gas[6,12,17] and wetted-wall tubes[3,18] have also been used to measure gas uptake by a liquid. In these systems, the gas flow through the tube is usually laminar, and diffusive transport of the trace gas to the wall occurs. Other methods of measuring accommodation coefficients and uptake coefficients were recently surveyed by Davis.[21]

There exists a large volume of literature on the use of flow tubes for reaction kinetics studies since Kaufman[22] published an extensive survey of reactions of oxygen atoms and described the equations governing diffusion with a first-order homogeneous reaction in the gas and heterogeneous reaction at the tube wall. Later, Howard[23] selectively surveyed the chemical kinetics literature associated with flow tube measurements and pointed out the need to take into account the effects of concentration gradients. He stated the relevant convective diffusion equation but did not develop a solution of it.

A somewhat more general form of the convection/reaction problem for laminar flow in a circular tube (Poiseuille flow) than that written by Kaufman is

$$2\langle v_G\rangle\left(1-\frac{r^2}{R^2}\right)\frac{\partial C_i}{\partial z}=D_{ij}\left[\frac{1}{r}\frac{\partial}{\partial r}\left(r\frac{\partial C_i}{\partial r}\right)+\frac{\partial^2 C_i}{\partial z^2}\right]-k_n C_i^n \qquad (1)$$

with boundary conditions at the tube centerline ($r = 0$) and tube wall ($r = R$) given by

$$\frac{\partial C_i}{\partial r}(0,z)=0 \quad D_{ij}\frac{\partial C_i}{\partial r}(a,z)=-k_W C_i(a,z) \qquad (2)$$

Here, $<v_G>$ is the mean velocity of the gas stream, R is the tube radius, C_i is the concentration of the reactive gas i, j refers to the carrier gas, z is the axial coordinate, r is the radial coordinate, D_{ij} is the gas-phase diffusion coefficient, and k_n is the nth-order reaction velocity constant. In Kaufman's formulation, $n = 1$, that is, the gas-phase reaction is first order, and the parameter k_W takes into account surface recombination of the reactive species and is given by

$$k_W=\gamma\frac{\bar{c}}{4} \qquad (3)$$

Here γ, the so-called uptake coefficient, is the fraction of molecular collisions with the wall leading to recombination of the reactive gas, $\bar{c}/4$ arises from the kinetic theory of gases for the molecular flux, and $\bar{c}$ is the mean molecular speed given by

$$\bar{c}=\sqrt{8k_B T/\pi m_i} \qquad (4)$$

in which k_B is Boltzmann's constant, T is the absolute temperature, and m_i is the molecular mass of the diffusing gas.

When axial diffusion is not negligible, two additional boundary conditions are needed to solve eq 1, and the difficulty associated with stating inlet conditions has not been generally recognized in the literature related to diffusion with chemical reaction in the tube flow. A more detailed discussion of this issue is given below.

10.1021/jp074939j CCC: $40.75
Published on Web 02/12/2008

Prior to Kaufman's extensive survey, Krongelb and Strandberg[24] studied atomic oxygen recombinations and modeled the combined diffusion and reaction problem assuming a second-order gas-phase reaction ($n = 2$ in eq 1) and neglecting axial diffusion. They assumed symmetry at the centerline of the tube and no mass flux at the wall ($k_W = 0$ in eq 2) and solved the governing equations with inlet condition

$$C_i(r, 0) = C_{i,0} \tag{5}$$

by a finite difference numerical method. They presented graphical results for the average concentration as a function of axial distance for various values of the parameter $D_{ij}/k_2C_{i,0}R^2$. Poirier and Carr[25] also used numerical methods to solve eq 1 for $n = 1$ and 2, neglecting axial diffusion, with boundary conditions of the form of eq 2. Although numerical solutions are required for $n > 1$ in eq 1, the problem for $n = 1$ can be solved analytically, that is, in terms of known special functions. It is difficult to apply published results using interpolation methods; therefore, alternate methods are desirable.

Judeikis[26] derived a traditional power series solution of the convective diffusion equation, eq 1 with $n = 1$, for the case of no reaction at the tube wall. He also obtained a solution for the case of flow in the annular region between two concentric cylindrical tubes. Donahue et al.[27] reported an approximate method for taking into account radial concentration gradients in flow reactors used to study free-radical kinetics. They considered the radicals to be introduced into the laminar flow at the centerline, forming an approximately Gaussian plume.

Convective diffusion problems of the type of eq 1 and its boundary conditions are often referred to as Graetz-like or extended Graetz problems stemming from Graetz's[28] analysis of the temperature distribution for laminar flow in a heated or cooled circular tube. There exists a very large amount of literature related to Graetz-like problems. Although most of the early work on the solution of Graetz problems involved numerical methods (e.g., Hsu[29] for heat transfer in a tube with axial conduction), a number of such problems can be solved in terms of well-known special functions. In the case of plug flow (uniform velocity), solutions can be obtained in terms of Bessel functions,[30] and for Poiseuille flow, solutions can be written in terms of the lesser known Kummer function (also called the confluent hypergeometric function). Abramowitz and Stegun[31] provided details of the properties (derivatives, integral representations, asymptotic expansions, zeros, etc.) of Kummer functions and tabulated them.

In studies of aerosol generation by the condensation of vapor in a flow tube, Nicolaon and his co-workers[32,33] obtained solutions for the temperature field in the cooled tube and the vapor concentration in terms of Kummer functions, and in 1972, Gershenzon et al.[30,34] solved two problems closely related to the analysis outlined here. Both solutions were developed in terms of the Kummer function. In the first problem, they solved eq 1 for a first-order gas-phase reaction with no wall loss ($k_W = 0$), and in the second paper, they solved eq 1 with $k_1 = 0$ using the boundary conditions given by eq 2.

More recently, Orkin et al.[35] applied the solution obtained by Gershenzon et al.[30] to estimate the error in the rate constant of a gas-phase reaction due to the parallel occurrence of a heterogeneous process.

A widely cited and applied analysis of kinetics measurements in a flow tube is that of Brown,[36] who developed an approximate solution for the concentration distribution of a reactive gas in a tubular laminar flow reactor undergoing a first-order reaction in the bulk gas and gas transport to the wall. He solved eq 1 (with $n = 1$) subject to boundary conditions given by eq 2, a problem previously analyzed by Walker.[37] Brown developed a simplification of Walker's asymptotic solution (valid for large z) of the equations using only the first term in an eigenfunction expansion using a power series in r/a to express the eigenfunction. He apparently was not aware of the work of Gershenzon and his co-workers;[30,34] therefore, he provided a simple numerical routine to calculate the relevant parameters. Because Brown's solution is only valid asymptotically, it cannot take into account possible radial variations in the inlet concentration of the reactive species and is not accurate for short tubes (or large gas flow rates). That is also the case for the solutions of Gershenzon et al.[30,34] and Orkin et al.,[35] who used only the first term in the solution of the full problem.

There is an additional difficulty associated with the solutions of Walker,[37] Brown,[36] Gershenzon et al.,[30,34] and others, who include axial diffusion in the analysis. These investigators assumed that at the point of introduction of the reactive gas ($z = 0$), the concentration can be specified a priori as $C_i(r,0)$. Since two boundary conditions are required in the axial direction, the second boundary condition was taken to be $C_i(r,\infty) = 0$. When axial diffusion is significant, diffusion in the $-z$ direction distorts the concentration distribution at $z = 0$. Furthermore, the inlet concentration distribution cannot be accurately represented by the asymptotic solutions obtained. These issues are addressed further below.

Additional numerical simulations for flow reactors were performed by Segatz et al.[38] for first-order kinetics in the bulk and at the wall. They briefly reviewed prior analyses and pointed out the need to consider the initial stage of the reaction.

In 1973, Davis[39] obtained solutions for a fairly wide class of Graetz-like problems in terms of the Kummer function. The methodology of Gershenzon et al.[30,34] and Davis[39] is used here to analyze transport and chemical reaction in tube flow. There is a need to re-examine the problem because many of the previous analyses are flawed, only approximate, or do not apply to short tubes and to inlet concentrations that are not spatially uniform. Furthermore, the flow field when there is a liquid film on the tube wall needs to be examined. A generalized solution in terms of well-known functions has considerable advantage to the user over numerical solutions carried out for specific cases.

Utter et al.[18] and Hanson et al.[3] used wetted-wall tubes to measure uptake coefficients, and they applied Brown's solution to interpret the data. Gershenzon et al.[40] also used flow tubes to measure uptake coefficients of HO_2 and CH_3O_2 on liquid surfaces of $H_2SO_4-H_2O$ and on salts. One flow tube they used extensively was a coaxial reactor with the aqueous solution or salt deposited on the cylinder wall. Magnetic resonance techniques were used to investigate the uptake. Recently, Aubin and Abbatt[41] reported on the use of a coated-wall flow tube to study the interaction of NO_2 with hydrocarbon soot. Initial uptake coefficients for three soot substances were found to be $(3.9 \pm 1.9) \times 10^{-5}$. They compared their results with numerous previously reported uptake coefficients that ranged from 10^{-8} to 0.1.

For the liquid film flow, Utter and his co-workers used results that apply to a thin falling film having no interfacial shear at the gas−liquid interface, and they estimated the film thickness based on such a theory. Analysis of their reported experimental conditions indicates that the gas flow rate was sufficiently large to produce significant interfacial shear. Consequently, the liquid film thicknesses were overestimated. It is useful to solve the co-current gas−liquid flow problem to determine the velocity

distributions in the gas and liquid phases before analyzing the gas-phase diffusion problem.

Analysis

For co-current downward laminar flow in a tube of radius R, the equations of motion for the gas and liquid flows are given by Bird et al.[42] and reduce to

$$\frac{\partial p}{\partial z} - \rho_G g = \mu_G\left[\frac{1}{r}\frac{\partial}{\partial r}\left(r\frac{\partial v_G}{\partial r}\right)\right] \quad (6)$$

and

$$\frac{\partial p}{\partial z} - \rho_L g = \mu_L\left[\frac{1}{r}\frac{\partial}{\partial r}\left(r\frac{\partial v_L}{\partial r}\right)\right] \quad (7)$$

in which $\partial p/\partial z$ is the pressure gradient, ρ_G and ρ_L and μ_G and μ_L are the gas and liquid densities and viscosities, respectively, g is the gravitational acceleration constant, and v_G and v_L are the gas and liquid velocities, which are considered to be functions of radial coordinate r only. It is assumed that both the gas and liquid flow rates are in the laminar flow regime.

The gas and liquid velocities are assumed to be independent of the axial direction because in trace gas experiments the concentration of the reacting species is very small compared with the carrier gas concentrations, and the carrier gases are not transferred to the liquid film nor the tube wall (in the absence of a liquid film). For example, in the wetted-wall uptake measurements of ozone on water reported by Utter et al.,[18] the inlet ozone concentration was $\sim 10^{11}$ molecules/cm^3, and the concentration of the carrier gas mixture (helium and water vapor) was $\sim 3.5 \times 10^{17}$ molecules/cm^3. Furthermore, the system was maintained at constant temperature; therefore, the densities of the gas and liquid did not change significantly (the pressure drop through the column was very small).

If the flow system is not isothermal or if the flow at the point of introducing the trace gas is not fully developed, the analysis of the flow field is much more complicated than that considered here. Khalizov et al.[43,44] used a computational fluid dynamics model to compute the flow field in laminar aerosol flow tubes. They showed that temperature gradients produce convection currents that lead to poorly defined residence times of the aerosol in the tube and that the design of the inlet to the flow tube has a large effect on the flow field.

If the liquid film thickness, δ, is uniform in the axial direction (neglecting ripples that can occur at higher flow rates), the boundary conditions are

$$\frac{\partial v_G}{\partial r}(0,z) = 0 \quad v_L(R,z) = 0 \quad v_G(R-\delta,z) = v_L(R-\delta,z) \quad (8)$$

and

$$\mu_G\frac{\partial v_G}{\partial r}(R-\delta,z) = \mu_L\frac{\partial v_L}{\partial r}(R-\delta,z) \quad (9)$$

The latter equation, eq 9, arises from the assumption that the shear stress is continuous across the gas−liquid interface located at $r = R - \delta$.

The solutions for this system of equations are

$$v_G = A(1-\sigma^2) + B\ln\sigma + C[\sigma^2 - (r/R)^2] \quad (10)$$

and

$$v_L = A[1-(r/R)^2] + B\ln(r/R) \quad (11)$$

where

$$A = \frac{\left(-\frac{\partial p}{\partial z} + \rho_L g\right)R^2}{4\mu_L} \quad B = \frac{(\rho_L - \rho_G)gR^2}{2\mu_L}$$

$$C = \frac{\left(-\frac{\partial p}{\partial z} + \rho_G g\right)R^2}{4\mu_G} \quad \sigma = 1 - \frac{\delta}{R} \quad (12)$$

The liquid volumetric flow rate is given by

$$Q_L = \left[\frac{(A-B)}{2} - \frac{A}{2}\sigma^2\right](1-\sigma^2) - B\sigma^2\ln\sigma \quad (13)$$

This nonlinear equation in the film thickness can be solved to determine the film thickness when the liquid flow rate is known. This result is substantially different than the result used by Utter et al.,[18] which is

$$Q_L = \frac{2\pi a\rho_L g\delta^3}{3\mu_L} \quad (14)$$

This equation is based on the flow of a thin film on a surface under the influence of gravity alone and does not take into account the axial pressure gradient and the interfacial shear exerted on the film by the gas flow. Consequently, it overpredicts the film thickness when there is significant interfacial shear.

When δ/R is sufficiently small ($\delta/R \ll 1$), which is the case in the experiments of Utter et al.[18] and Hanson et al.,[3] the gas-phase velocity distribution reduces to the classical Poiseuille flow velocity distribution

$$v_G = C[1-(r/R)^2] \quad (15)$$

and the mean gas velocity becomes

$$\langle v_G\rangle = \frac{1}{2}v_{G,max} = \frac{1}{2}C = \frac{(-\partial p/\partial z + \rho_G g)R^2}{8\mu_G} \quad (16)$$

Thus, in the limit of small δ/R, the velocity distribution is that used in the convection term in eq 1. Of course, in the absence of a liquid film on the wall, the gas flow is Poiseuille flow for laminar flow conditions.

It is convenient to write the governing equations in nondimensional form by introducing the following variables and parameters

$$\phi = C_i/\langle C_{i,0}\rangle \quad \eta = r/R \quad \zeta = z/R\mathrm{Pe} \quad \mathrm{Pe} = 2R\langle v_G\rangle/D_{ij} \quad (17)$$

Here, $\langle C_{i,0}\rangle$ is the inlet trace gas concentration averaged over the cross-sectional area of the gas, and Pe is the Peclet number for mass transfer. In the ideal case, $\langle C_{i,0}\rangle$ is simply the inlet concentration, but if the inlet concentration is not radially uniform, $\langle C_{i,0}\rangle$ must be calculated based on knowledge of the radial distribution. The Peclet number is a measure of the rate of axial transport of the trace gas to the axial transport by molecular diffusion.

The convective diffusion equation for a first-order reaction in the bulk gas transforms to

$$(1-\eta^2)\frac{\partial\phi}{\partial\zeta} = \frac{1}{\eta}\frac{\partial}{\partial\eta}\left(\eta\frac{\partial\phi}{\partial\eta}\right) + \frac{1}{\mathrm{Pe}^2}\frac{\partial^2\phi}{\partial\zeta^2} - \mathrm{Da}\phi \quad (18)$$

in which Da is a Damkohler number defined by

$$\mathrm{Da} = kR^2/D_{ij} \tag{19}$$

which is the ratio of the diffusion time to the reaction time (or a ratio of the chemical reaction rate to the molecular diffusion rate). If there is no bulk reaction in the gas, Da = 0.

The convective diffusion equation must be solved subject to appropriate boundary conditions. The boundary conditions at the centerline and wall given by eq 2 transform to

$$\frac{\partial \phi}{\partial \eta}(0,\zeta) = 0 \quad \frac{\partial \phi}{\partial \eta}(1,\zeta) = -\kappa\phi(1,\zeta) \tag{20}$$

in which

$$\kappa = R\gamma\bar{c}/4D_{ij} \tag{21}$$

In most of the previous analyses of diffusion and reaction in flow tubes, the authors apply an entry condition based on the assumption of a uniform inlet concentration of reactive gas. Although this is a reasonable condition for large Peclet numbers, when axial diffusion cannot be neglected (small Pe), two boundary conditions in the axial direction are required for a well-posed problem. For low Pe, axial diffusion affects both the upstream ($\zeta < 0$) and downstream ($\zeta > 0$) concentration distributions. Consequently, the concentration at $\zeta = 0$ cannot be specified a priori. Papoutsakis et al.[45,46] and Acrivos[47] addressed this issue for the extended Graetz problem associated with laminar flow heat transfer. Papoutsakis and his co-workers[45] solved the constant wall temperature (for $\zeta > 0$) extended Graetz problem and the constant wall flux problem,[46] and Acrivos provided the corresponding asymptotic solution for $\mathrm{Pe_H} \ll 1$, where the Peclet number for heat transfer is analogous to the Peclet number for mass transfer and is defined by $\mathrm{Pe_H} = 2R\langle v\rangle/\alpha_H$, in which α_H is the thermal diffusivity. In these analyses, the wall temperature was considered to be uniform for $\zeta \rightarrow \infty$.

For low $\mathrm{Pe_H}$, the temperature distribution (or concentration distribution in the analogous mass-transfer problem) is significantly distorted from a uniform distribution near the wall ($\eta >$ 0.5), where axial diffusion is more pronounced compared with the convective transport of the fluid. The results of Papoutsakis et al.[45,46] demonstrate that for $\mathrm{Pe_H} \geq 10$, the uniform temperature profile is established within very small negative values of ζ. For example, their results show that for $\mathrm{Pe_H} = 10$, it takes only 25% of the tube diameter upstream for the uniform temperature profile to be established, and they concluded that axial conduction (or diffusion) is negligible if $\mathrm{Pe_H} > 50$.

The Peclet numbers associated with the experiments of Utter et al.[18] and Hanson et al.[3] generally exceed 50; therefore, axial diffusion could be neglected. In this case, only one additional boundary condition is required, which, in general, may be written as

$$\phi(\eta,0) = \frac{C_i(\eta,0)}{\langle C_i(\eta,0)\rangle} \tag{22}$$

where $C_i(\eta,0)$ is the inlet concentration distribution written in terms of dimensionless radius η.

For instantaneous reaction at the gas−liquid surface (or wall), $\phi(1,\zeta) = 0$. This problem corresponds to the classical dimensionless Graetz problem[28] for heat transfer in fully developed laminar flow with constant wall temperature. In most texts, the Graetz problem is solved by applying the method of separation of variables using numerical methods to obtain the relevant eigenfunctions, but here, we develop the solution in terms of Kummer functions.

To solve eq 18, neglecting axial diffusion, let $\phi(\eta,\zeta)$ be the product $f(\zeta)g(\eta)$, in which $f(\zeta)$ is an exponential function

$$f(\zeta) = E\exp(-\lambda^2\zeta) \tag{23}$$

and $g(\eta)$ satisfies the Sturm−Liouville equation

$$\frac{\mathrm{d}}{\mathrm{d}\eta}\left(\eta\frac{\mathrm{d}g}{\mathrm{d}\eta}\right) + [\eta(1-\eta^2)\lambda^2 - \mathrm{Da}\eta]g = 0 \tag{24}$$

where E and λ are constants to be determined, and the boundary conditions become

$$\frac{\mathrm{d}g}{\mathrm{d}\eta}(0) = 0 \quad \frac{\mathrm{d}g}{\mathrm{d}\eta}(1) = -\kappa g(1) \tag{25}$$

This system of equations constitutes a Sturm−Liouville problem. Consequently, there exists an infinite set of orthogonal functions, $g_n(\eta)$, that satisfies the Sturm−Liouville equation.

In their solution of eq 18 including axial diffusion, Walker,[37] Brown,[36] and Gershenzon and his co-workers,[30,34] assumed that $f(\zeta)$ is given by eq 23. With this assumption, the product solution yields

$$\frac{\mathrm{d}}{\mathrm{d}\eta}\left(\eta\frac{\mathrm{d}g}{\mathrm{d}\eta}\right) + [\eta(1-\eta^2)\lambda^2 - \mathrm{Da}\eta + \lambda^3/\mathrm{Pe}^2]g = 0 \tag{26}$$

which is not a Sturm−Liouville equation. This has a significant effect related to satisfying the inlet condition.

Introducing the transformations[39]

$$t = \lambda\eta^2 \quad \text{and} \quad w = \exp(\lambda\eta^2/2)g(\eta) \tag{27}$$

eq 24 transforms to Kummer's equation[31]

$$t\frac{\mathrm{d}^2w}{\mathrm{d}t^2} + (\beta - t) - \alpha w = 0 \tag{28}$$

with

$$\alpha = (2 - \lambda + \mathrm{Da}/\lambda)/4 \quad \text{and} \quad \beta = 1 \tag{29}$$

The relevant solution of Kummer's equation here is the confluent hypergeometric function (also called the Kummer function), $M(\alpha,\beta,t)$, defined by

$$M(\alpha,\beta,t) = 1 + \frac{\alpha}{\beta}\frac{t}{1!} + \frac{\alpha(\alpha+1)}{\beta(\beta+1)}\frac{x^2}{2!} + \frac{\alpha(\alpha+1)(\alpha+2)}{\beta(\beta+1)(\beta+2)}\frac{x^3}{3!} + \ldots \tag{30}$$

Only one solution of eq 28 is needed because the transformations leading to it automatically satisfy the boundary condition at $\eta = 0$. Consequently, the solution becomes

$$g_n(\eta) = \exp(-\lambda_n\eta^2/2)M\left(\frac{(2 - \lambda_n + \mathrm{Da}/\lambda_n)}{4}, 1, \lambda_n\eta^2\right) \tag{31}$$

The confluent hypergeometric function has properties described by Abramowitz and Stegun[31] and numerous mathematical texts and was tabulated by Abramowitz and Stegun. The most relevant property needed here is the derivative

$$\frac{\mathrm{d}}{\mathrm{d}t}M(\alpha,\beta,t) = \frac{\alpha}{\beta}M(\alpha+1,\beta+1,t) \tag{32}$$

If the transformations given by eq 27 are applied to the full problem including axial diffusion, one obtains the solution for

$g_n(\eta)$ given by Gershenzon et al.[30] for the case of no wall loss, which is

$$g_n(\eta) = \exp(-\lambda_n\eta^2/2)M\left(\frac{(2-\lambda_n+\mathrm{Da}/\lambda_n-\lambda_n^3/\mathrm{Pe}^2)}{4},1,\lambda_n\eta^2\right) \quad (33)$$

For large Pe, this reduces to eq 31. They considered only the smallest positive value of λ_n, that is, λ_1.

Using eq 31, the boundary condition at $\eta = 1$ and the derivative property, the eigenvalues, λ_n, satisfy

$$(\kappa-\lambda_n)M\left(\frac{\left(2-\lambda_n+\frac{\mathrm{Da}}{\lambda_n}\right)}{4},1,\lambda_n\right)+\lambda_n\left(2-\lambda_n+\frac{\mathrm{Da}}{\lambda_n}\right)M\left(\frac{\left(6-\lambda_n+\frac{\mathrm{Da}}{\lambda_n}\right)}{4},2,\lambda_n\right)=0 \quad (34)$$

If Da/λ_n is replaced by $\mathrm{Da}/\lambda_n - \lambda_n^3/\mathrm{Pe}^2$ and $\kappa = 0$, the solution of Gershenzon et al.[30] is obtained. If there is no bulk reaction and Da/λ_n is replaced by $-\lambda_n^3/\mathrm{Pe}^2$, the second solution considered by Gershenzon et al.[34] is recovered.

By superposition of solutions, the full solution becomes

$$\phi(\eta,\xi) = \sum_{n=1}^{\infty} E_n \exp(-\lambda_n^2\xi)g_n(\eta) \quad (35)$$

and the constants E_n are obtained from the initial condition by applying the orthogonality of the eigenfunctions, that is

$$\int_0^1 \eta(1-\eta^2)g_m(\eta)g_n(\eta)\mathrm{d}\eta = \begin{cases} 0 \text{ for } m \neq n \\ ||g_n(\eta)||^2 \text{ for } m = n \end{cases} \quad (36)$$

where

$$||g_n(\eta)||^2 = \int_0^1 \eta(1-\eta^2)[g_n(\eta)]^2\mathrm{d}\eta \quad (37)$$

When the axial diffusion term is not negligible, the functions $g_n(\eta)$ given by eq 33 are not orthogonal. This was shown by Davis and Bonano[48] for the similar problem of mass transfer to a laminar falling film and by Papoutsakis and his co-workers[45,46] for the extended Graetz problem. Consequently, the following steps needed to obtain the coefficients E_n in the analysis cannot be applied unless axial diffusion is negligible.

Using eq 35, the initial condition, eq 22, can be expanded in an eigenfunction expansion as follows

$$\phi(\eta,0) = \frac{C_i(\eta,0)}{\langle C_i(\eta,0)\rangle} = \sum_{n=1}^{\infty} E_n g_n(\eta) \quad (38)$$

where the coefficients E_n are obtained by applying orthogonality, that is

$$E_n = \frac{1}{||g_n(\eta)||^2}\int_0^1 \eta(1-\eta^2)\frac{C_i(\eta,0)}{\langle C_i(\eta,0)\rangle}g_n(\eta)\mathrm{d}\eta \quad (39)$$

In general, this result cannot be integrated until $C_i(\eta,0)$ is specified. For example, Donahue et al.[27] assumed the inlet concentration distribution to be roughly Gaussian.

Utter et al.,[18] Hanson et al.,[3] Thornton and Abbatt,[6] and Hanson and Ravishankara[12] introduced the trace gas through a glass injector that could be moved in the z direction. An approximation for the inlet concentration distribution for a circular tube with inner radius R having a cylindrical injector with inner radius R_0 inserted along the centerline can be applied if the injector flow rate, Q_0, the total flow rate in the tube, Q, and the inlet concentration in the injector, $C_{i,0}$, are known. In this case, the concentration distribution is given by

$$C_i(\eta,0) = \begin{Bmatrix} C_{i,0} \text{ for } 0 \le \eta \le R_0/R \\ 0 \text{ for } R_0/R \le \eta \le 1 \end{Bmatrix} \quad (40)$$

and the mean inlet concentration due to dilution of the trace gas in the carrier gas stream becomes

$$\langle C_i(0)\rangle = (Q_0/Q)C_{i,0} \quad (41)$$

Hanson et al.[3] reported the outer diameter of the injector to be 10 mm ($R_0 \sim 4$ mm for a 1 mm tube wall thickness) in reference 18 and 9 mm ($R_0 \sim 3.5$ mm) in reference 3, and the flow tube i.d. was 25.4 mm ($R = 12.7$ mm), but the flow rate Q_0 was not specified. Thornton and Abbatt[6] used a 6 mm o.d. ($R_0 \sim 2$ mm) injector in a 60 mm i.d. ($R = 30$ mm) flow tube. They reported the flow rates to be $Q_0 = 2500$ slpm and $Q = 7600$ slpm, respectively. In both studies, the inlet concentration was not measured.

The injector design has two major effects on the interpretation of data. As discussed above, the first is that the inlet concentration distribution is spatially nonuniform, and the second is that the assumed parabolic velocity profile of the carrier gas is distorted in the region near the injector. This is particularly a problem with the high flow rate through the small injector used by Thornton and Abbatt[6] because the injector produced a jet of fluid at the centerline of the flow.

If the concentration distribution given by eq 40 can be applied, the coefficients E_n are given by

$$E_n = \frac{Q}{Q_0||g_n(\eta)||^2}\int_0^{R_0/R} \eta(1-\eta^2)g_n(\eta)\mathrm{d}\eta \quad (42)$$

In the absence of detailed information on the inlet concentration distribution, the assumption of a spatially uniform distribution is a very rough approximation that can be adapted to analyze data, provided that the data can be extrapolated to yield an estimate of the mean inlet concentration. This does not lead to large error downstream of the inlet region where the concentration is not sensitive to the inlet value.

Taking the inlet concentration to be uniform at the radial-average concentration, $C_i(\eta,0)/\langle C_i(\eta,0)\rangle = 1$, the coefficients E_n become

$$E_n = \frac{1}{\lambda_n^2||g_n(\eta)||^2}\left[\mathrm{Da}I_1 - \frac{\mathrm{d}g_n}{\mathrm{d}\eta}(1)\right] \quad (43)$$

where I_1 is the integral

$$I_1 = \int_0^1 \eta g_n(\eta)\mathrm{d}\eta \quad (44)$$

which is readily calculated using MatLab or other software. The zeros of eq 34, the integrals and derivatives involving $M(\alpha,\beta,t)$, were calculated using MatLab in this study. For such computations, it is useful to write the Kummer function in the form

$$M(\alpha,\beta,t) = 1 + \frac{\alpha}{\beta}\frac{t}{1}\left\{1 + \frac{(\alpha+1)}{(\beta+1)}\frac{t}{2}\left[1 + \frac{(\alpha+2)}{(\beta+2)}\frac{t}{3}\right]\cdots\left(1 + \frac{(\alpha+N)}{(\beta+N)}\frac{t}{N}\right)\right\} \quad (45)$$

where N is taken to be sufficiently large such that $(\alpha + N)t/(\beta + N)N \ll 1$.

Results

In addition to the general case of bulk reaction and wall loss, two limiting cases are of some interest, as indicated by the analyses of Gershenzon et al.[30,34] and others discussed above; these are (i) bulk chemical reaction with no wall loss and (ii) no bulk chemical reaction with instantaneous reaction at the wall. It is convenient to present graphical results in terms of the dimensionless mixed mean concentration $\langle\phi(\zeta)\rangle$ obtained by averaging $\phi(\eta,\zeta)$ over the cross-sectional area of the gas to give

$$\langle\phi(\zeta)\rangle = 4\sum_{n=1}^{\infty}\frac{E_n}{\lambda_n^2}\exp(-\lambda_n^2\zeta)\left[\mathrm{Da}I_1 - \frac{\mathrm{d}g_n}{\mathrm{d}\eta}(1)\right] \quad (46)$$

When there is no wall loss, $\mathrm{d}g_n/\mathrm{d}\eta = 0$ at $\eta = 1$. For this case, Table 1 lists the first five eigenvalues for various values of the Damkohler number, and Figure 1 shows the effect of Da on the dimensionless mean concentration. For Da > 3, the reaction goes to completion within the dimensionless axial distance $\zeta < 1$. Clearly, the Damkohler number has a large effect on the extent of the reaction.

In the absence of bulk-phase reaction (Da = 0), the decay in the mean concentration is governed by the dimensionless uptake parameter κ. Table 2 lists the first five eigenvalues for various values of κ.

The application of this analysis to diffusion and reaction in flow tubes involves several dimensionless parameters; the Peclet number (Pe), the Damkohler number (Da), and the wall reaction parameter (κ) appear explicitly in the analysis, and the Sherwood number (Sh) and Nusselt number (Nu) are determined in the analyses of mass-transfer and heat-transfer processes. In addition, the gas and liquid Reynolds numbers, $\mathrm{Re_G}$ and $\mathrm{Re_L}$ must be taken into account in the interpretation of data. Table 3 lists the various dimensionless groups, their definitions, and their significance. More extensive lists of dimensionless groups encountered in various branches of engineering, physics, and chemistry were published by Boucher and Alves.[49,50]

Application to Aerosol Flow Tubes. Thornton and Abbatt[6] reported data for the uptake of HO_2 to Cu(II)-doped H_2SO_4/H_2O aerosol at 35% relative humidity (RH) and to NH_4HSO_4/H_2O aerosol at 42% RH. They also performed experiments in the absence of aerosol to determine if wall losses contributed significantly to the decay in the HO_2 signal and without doping to determine the effect of the Henry's law constant on the uptake. The submicrometer aerosol droplets were entrained in the flow through a circular tube having a diameter of 6 cm, and the system was operated at atmospheric pressure (755 Torr) and room temperature (295 K). The flow system was coupled to a chemical ionization mass spectrometer to determine the loss of HO_2. They found the wall loss to be very small compared with the uptake by the aerosol. The gas Reynolds number was approximately 200, $<\upsilon_G> \approx 4.5$ cm/s, and they took $D_G = 0.25$ cm^2/s. This corresponds to a Peclet number of approximately 100; therefore, axial diffusion can be neglected.

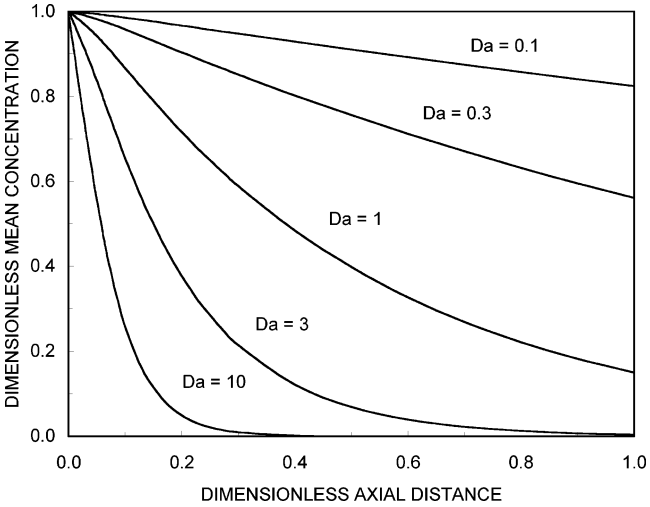

Figure 1. The effect of the Damkohler number on the axial mean concentration distribution.

TABLE 1: Eigenvalues for Various Damkohler Numbers and No Wall Loss ($\kappa = 0$) Computed by Finding the Zeros of Eq 34

Da =	0.1	0.3	1	3	10
λ_1 =	0.4467	0.7722	1.3998	2.3778	4.1059
λ_2 =	5.0872	5.1265	5.2621	5.635	6.7799
λ_3 =	9.1685	9.1903	9.2664	9.4819	10.2103
λ_4 =	13.2048	13.2199	13.2729	13.4237	13.9449
λ_5 =	17.2260	17.2376	17.2783	17.3942	17.7976

TABLE 2: Eigenvalues for Various Values of κ and No Bulk Chemical Reaction (Da = 0) Computed by Finding the Zeros of Eq 34

K =	0.1	1	10	100	1000	∞
λ_1 =	0.6183	1.6412	2.5168	2.6843	2.7023	2.7043
λ_2 =	5.1169	5.4783	6.3646	6.6432	6.6754	6.679
λ_3 =	9.1889	9.436	10.2707	10.6249	10.6684	10.6733
λ_4 =	13.2211	13.4152	14.2002	14.6116	14.665	14.671
λ_5 =	17.2399	17.4026	18.1437	18.6004	18.6627	18.6698

TABLE 3: Dimensionless Groups Encountered in Heat and Mass Transfer Associated with Flow Tubes

symbol	name	definition	significance
Da	Damkohler number	kR^2/D_{ij}	chemical reaction rate/ molecular diffusion rate
Nu	Nusselt number	$2Rh/k_{heat}$	total heat transfer/ conductive heat transfer
Pe	mass-transfer Peclet number	$2R\langle\upsilon\rangle/D_{ij}$	bulk transport of mass/ diffusive transport of mass
$\mathrm{Pe_H}$	heat-transfer Peclet number	$2R\langle\upsilon\rangle/\alpha_{heat}$	bulk transport of heat/ conductive transport of heat
$\mathrm{Re_G}$	gas-phase Reynolds number	$2R\rho_G\langle\upsilon_G\rangle/\mu_G$	inertial force of gas/ viscous force of gas
$\mathrm{Re_L}$	liquid-phase Reynolds number	$\delta\rho_L\langle\upsilon_L\rangle/\mu_L$	inertial force of liquid/ viscous force of liquid
Sh	Sherwood number	$2RK/D_{ij}$	total mass transfer/ molecular diffusion
κ	interfacial reaction number	$R\gamma\bar{c}/4D_{ij}$	interfacial decomposition rate/ molecular diffusion rate

The HO_2 concentration was measured relatively far from the injector inlet, and they reported relative distances. The shortest distance in each set of measurements was taken 20−30 cm downstream of the injector inlet. For the calculations discussed below, the shortest distance was taken to be 25 cm from the inlet, and the approximate inlet concentration was obtained by extrapolating the data to the inlet.

Figure 2 compares the data for HO_2 decay in the absence of any aerosol with the analysis developed here assuming a first-order reaction in the bulk gas and no wall loss. The data

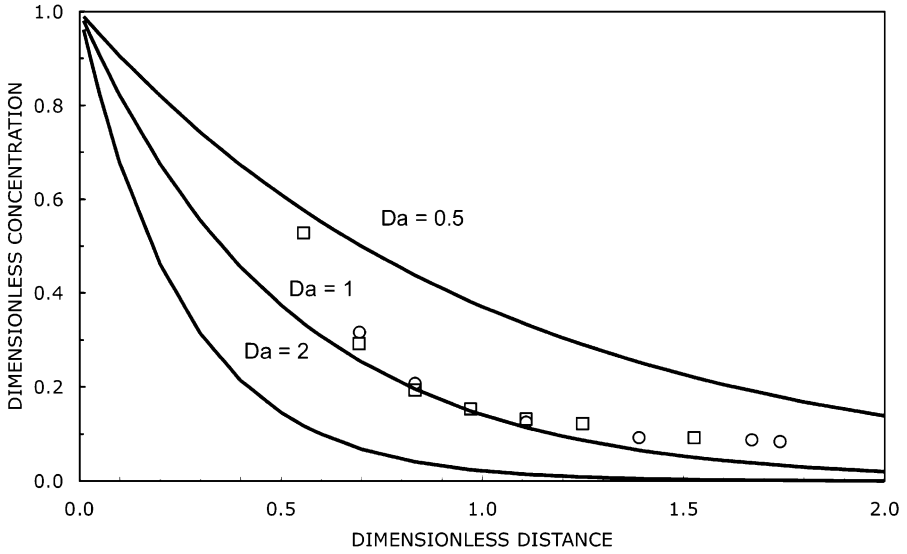

Figure 2. The gas-phase HO_2 decay data of Thornton and Abbatt[6] from their Figure 1 (□) and Figure 2 (○) compared with this analysis for various Damkohler numbers.

correspond to those in Figures 1a and 2 in ref 6. The aerosol-free data of Figures 1 and 2 of the authors are in very good mutual agreement in nondimensional parameters, and they best agree with the analysis for Da = 1, which yields a first-order reaction rate constant $k_1 = 0.028\ s^{-1}$. The HO_2 decay is seen to decrease more rapidly than that calculated for a first-order reaction, which suggests that a first-order reaction is not a reasonable assumption. Thornton and Abbatt[6] considered the gas-phase decay to be second order in HO_2.

Transport to a Tube Wall. The limiting case of an instantaneous reaction at the wall, which corresponds to the maximum possible mass flux to the surface, can be illustrated by computing the interfacial mass flux defined by

$$j|_{r=a} = -D_{ij}\frac{\partial C_i}{\partial r}(R,z) = K_G[\langle C_i(z)\rangle - 0] \qquad (47)$$

where K_G is a gas-phase mass-transfer coefficient and $<C_i(z)>$ is the bulk mean concentration of the diffusing species. The zero signifies that the concentration at the interface vanishes because of the instantaneous reaction. This limiting case corresponds to $\gamma = \infty$ ($\kappa = \infty$) in Brown's problem.

In nondimensional form, the mass flux equation is

$$-\frac{\partial \phi}{\partial \eta}(1,z) = \frac{\mathrm{Sh}}{2}\langle \phi(\zeta)\rangle \qquad (48)$$

in which Sh is the Sherwood number (dimensionless mass-transfer coefficient) defined by

$$\mathrm{Sh} = 2RK_G/D_{ij} \qquad (49)$$

Since $\phi(\eta,\zeta)$, its derivative, and its mean value $<\phi(\zeta)>$ can be calculated from the solution developed above, the Sherwood number can be determined. The result is presented in Figure 3. The Sherwood number decreases from infinity at $\zeta = 0$ to an asymptotic value $\mathrm{Sh}_\infty = \lambda_1^2/2 = 3.6568$ within a dimensionless distance of $\zeta \sim 0.1$. This region can be considered to be an entry region or transition region in which the mass flux varies significantly with axial distance ζ. The asymptotic Sherwood number is identical to the asymptotic Nusselt number, Nu_∞, obtained for the analogous heat-transfer problem[28] and the Sherwood number reported by Gershenzon et al.[7] for a cylindrical reactor. The Nusselt number is defined by $\mathrm{Nu} = 2Rh/k_{heat}$, in which h is a heat-transfer coefficient analogous to the mass-transfer coefficient defined by eq 48 and k_{heat} is the thermal conductivity of the fluid. The asymptotic Nusselt number of 3.6568, which applies for large Pe, can be compared with the asymptotic Nusselt numbers calculated by Papoutsakis et al.[45] for various Pe. For Pe = 5, they obtained $\mathrm{Nu}_\infty = 3.778$, and for Pe = 10, they reported $\mathrm{Nu}_\infty = 3.695$. Consequently, the effect of the Peclet number on the radial transport is not great for Pe > 10.

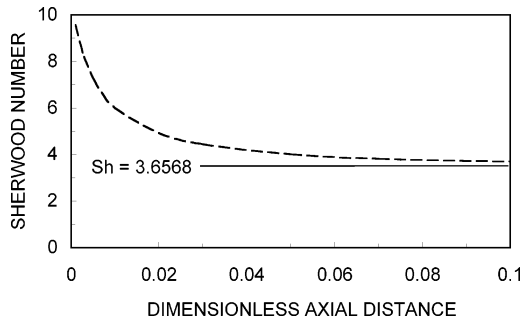

Figure 3. The Sherwood number in the transition region (- - -) and the asymptotic Sherwood number (——).

For $\zeta < 0.05$, the mass flux at the interface is much larger than the asymptotic value, and in this region, the number of terms in the series representing the solution for $\phi(\eta,\zeta)$ increases as ζ decreases. In the region of practical interest, five terms have been found to be adequate, and in the asymptotic region, only one term is needed. Note that the solutions of Walker,[37] Brown,[36] and Gershenzon et al.[30,34] correspond to using the first term of eq 35. For $\zeta = 0.01$, the Sherwood number given by using the full solution is 5.9900 whereas the previous analyses yield Sh = 3.6568. Since the mass flux to the wall is proportional to the Sherwood number, the mass flux is greatly underestimated using a single term.

When $\kappa < \infty$, it is not convenient to express results in terms of a Sherwood number. It is more appropriate to calculate the mixed mean concentration of the trace gas (either $\langle C_i(z)\rangle$ or $\langle \phi(\zeta)\rangle$) that depends on the axial distance. The first step is the calculation of the eigenvalues λ_n, and the eigenvalues listed in Table 2 have been used to calculate the eigenfunctions and dimensionless concentrations.

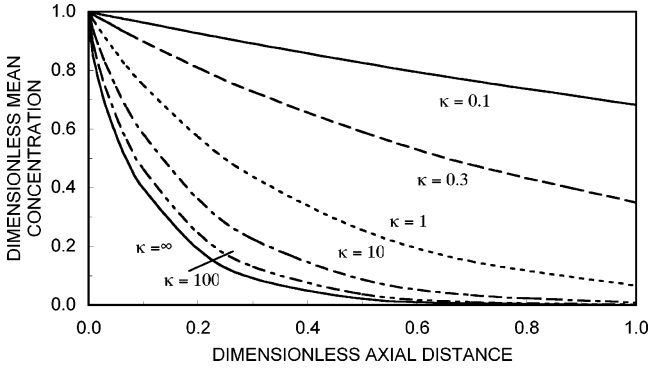

Figure 4. The effects of the dimensionless uptake coefficient κ on the trace gas mean concentration profile.

TABLE 4: The Parameters Reported by Utter et al. for the Uptake of Ozone by a Film of Water

temperature	total pressure	length of absorber
$T = 276$ K	$P_{total} = 10.85$ Torr	$L = 60$ cm
tube radius	film thickness	inlet ozone concentration
$R = 1.27$ cm	$\delta = 0.02$ cm	$C_{i,0} = 10^{11}$ molecules/cm^3
mean gas velocity	gas-phase diffusivity	carrier gases
$<v_G> = 457$ cm/s	16 cm^2/s	H_2O and He

Figure 4 shows how the dimensionless uptake coefficient κ affects the mixed mean concentration. For $\kappa > 10$, the mean concentration profile deviates little from the limiting case of large κ, but at lower uptake coefficients, the axial distribution is very sensitive to κ (or γ).

Application to Wetted-Wall Tubes. Utter et al. provided one complete set of uptake data for O_3 uptake on water that could be analyzed using the method outlined above. Table 4 lists the relevant parameters for an experiment in which Na_2SO_3 was used as a scavenger for the uptake of O_3. The gas and liquid flows were both laminar, but some rippling was encountered. The effects of ripples have not been taken into account in the above analysis of the flow fields.

Figure 5 shows a comparison between the data of Utter et al. and computed results for two values of the uptake coefficient, $\gamma = 0.0008$ and 0.001 using $D_{ij} = 16$ cm^2/s, which is the gas-phase diffusivity reported by the authors. Also shown for reference is the curve calculated for $\gamma = 1$. The data are in good agreement with the results for $\gamma = 0.0008$. An independent calculation of the gas-phase diffusivity for ozone in a mixture of water vapor and helium using the Chapman−Enskog theory discussed by Bird et al.[42] yields $D_{ij} = 13$ cm^2/s. For this lower value of the diffusivity, the Peclet number is increased, and the data are shifted to smaller dimensionless axial distances. Utter et al. reported $\gamma = 0.00076$ for this set of data using Brown's analysis. The agreement between the present analysis and that of Brown is due to the fact that at the relatively low gas flow rates (or Peclet numbers) used by the authors, most of the tube length corresponds to the asymptotic mass-transfer region where only the first term of the infinite series is needed. That is not generally the case for the experiments of Hanson and his coworkers.[3]

Figures 6−9 compare the wetted-wall data of Hanson et al.[3] with the analysis described here. Note that many of the data points are at dimensionless axial distances lower than those of Utter et al. because of the much higher gas velocities. Consequently, much of the data is in the transition region (or entry region) where Brown's analysis[36] is not accurate. The gas-phase diffusivities reported by the authors were used for each calculation of the axial concentration distribution. Each of the figures has an insert that shows the original graphs and the mean gas velocities. The dimensionless variables used here tend to consolidate the data.

Hanson et al.[3] plotted their data in terms of a relative position of the detector. To estimate the position relative to the inlet and the inlet mean concentration, the data in the various sets of data were extrapolated to yield the same position and inlet concentration for each data set. For example, for the inset of Figure 6 (Figure 1a of the authors), the inlet is estimated to be at −20 cm based on the relative positions shown in the figure.

For the OH radical uptake on water shown in Figure 6, the data scatter about the curve corresponding to $\gamma_{OH} = 1$. Also shown in the plot are the calculated results for $\gamma_{OH} = 0.1$, which nearly fall on the curve for $\gamma_{OH} = 1$. The data for the lowest gas velocity suggest that γ_{OH} could be as low as 0.1. The data which fall to the left of the curve for $\gamma = 1$ correspond to the two higher flow rates where more pronounced rippling would occur. Using Brown's[36] analysis, the authors reported $\gamma_{OH} = 0.0035$ for OH on water.

The results for the uptake of OH radicals on H_2SO_4 presented in Figure 7 show much more scatter than any of the other data sets. The data obtained at the highest gas velocity ($<v_G> = 4220$ cm/s) fall near the curve for $\gamma_{OH} = 0.008$, and the results for the lowest gas velocity ($<v_G> = 2560$ cm/s) agree with the analysis for $\gamma_{OH} = 0.04$. The authors reported $\gamma_{OH} > 0.08$ for H_2SO_4.

The results for HO_2 radicals on water shown in Figure 8 are reasonably well consolidated and fall in the range of $0.01 < \gamma_{HO_2} < 1$. The data for HO_2 radicals on H_2SO_4, presented in Figure 9, show the best consolidation achieved by nondimensionalizing the concentrations and positions, and the data scatter about the calculated results for $\gamma_{HO_2} = 0.03$.

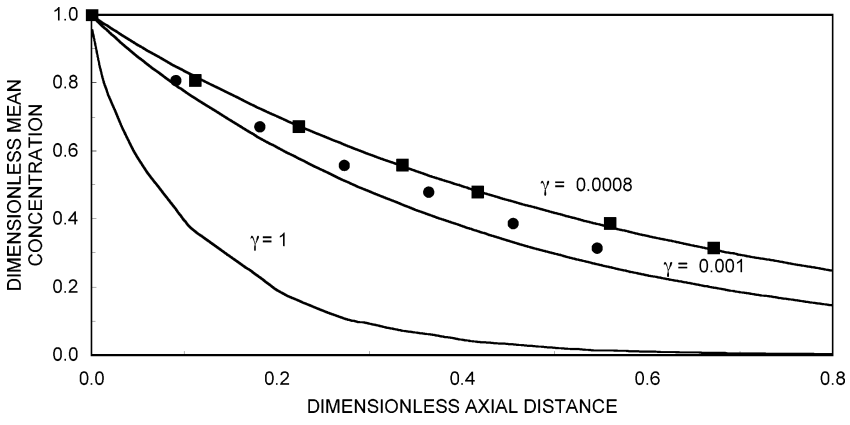

Figure 5. The ozone uptake data of Utter et al.[18] compared with the wetted-wall tube analysis for $D_{ij} = 16$ cm^2/s (ν) and 13 cm^2/s (λ).

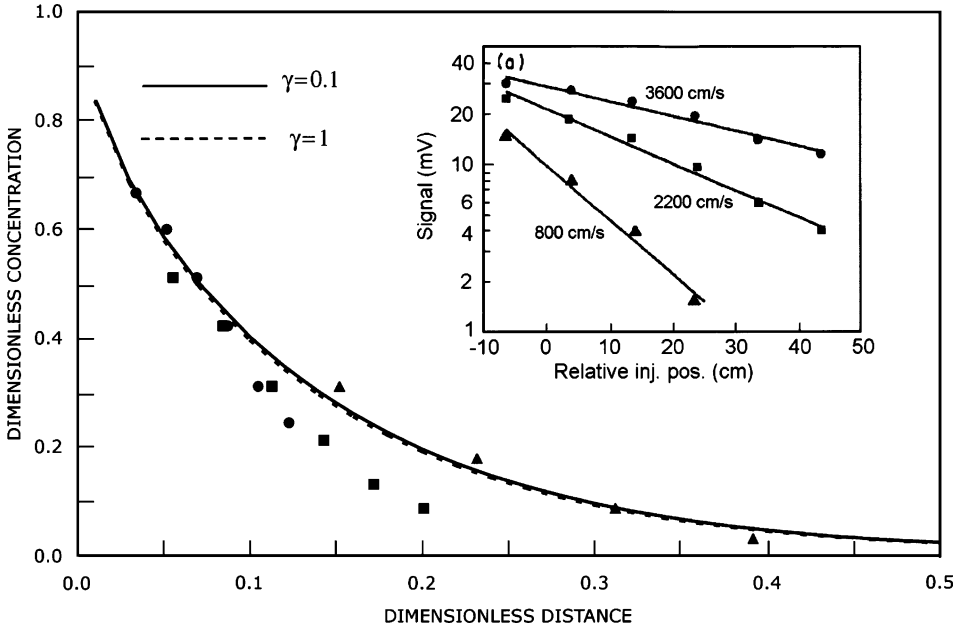

Figure 6. The OH/H_2O data of Hanson et al.[3] compared with the wetted-wall tube analysis. The inset is a redrawing of the original graph of the investigators.

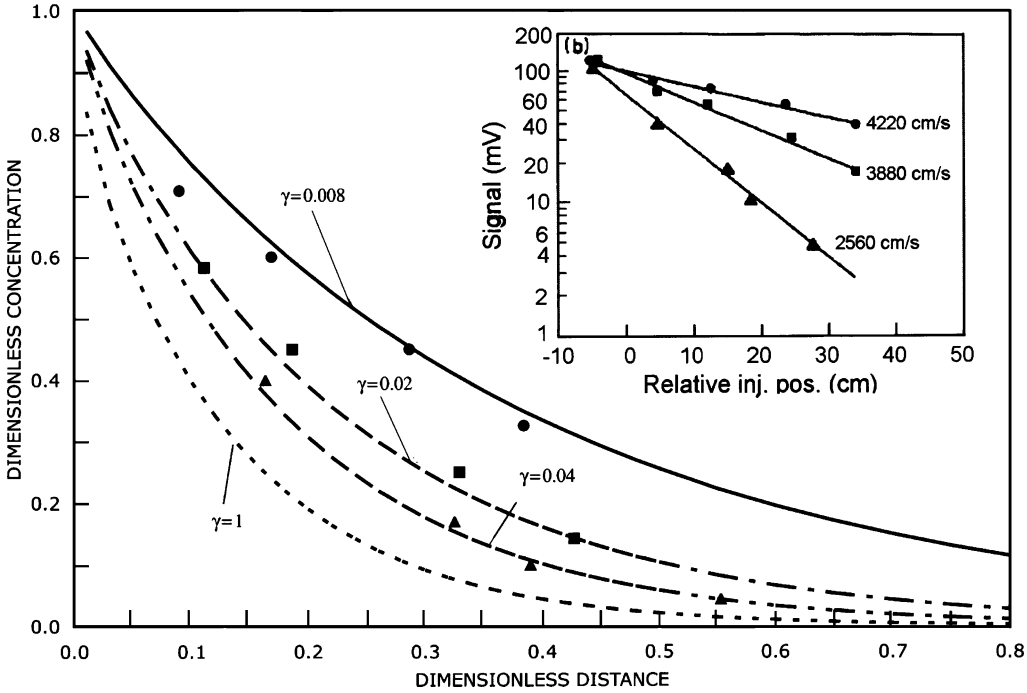

Figure 7. The OH/H_2SO_4 data of Hanson et al.[3] compared with the wetted-wall tube analysis. The inset is a redrawing of the original graph of the investigators.

The authors reported $\gamma_{HO_2} > 0.01$ for water and $\gamma_{HO_2} > 0.05$ for H_2SO_4, which is consistent with the results found here. Because the results obtained from the convective diffusion theory are not very sensitive to γ in the range of $0.05 < \gamma < 1$, experimental measurements cannot be expected to yield highly accurate results in this range.

Discussion

The analysis of the effects of diffusion on the transport of a trace gas to a tube wall or liquid interface developed here effectively consolidates data obtained by varying the gas flow rate and other experimental parameters. Furthermore, the effect of a first-order chemical reaction in the bulk gas can be taken into account. The parametric study represented by Figure 4 shows that the mixed mean concentration distribution is not sensitive to the dimensionless uptake parameter κ for large values of κ, and it is very sensitive to the gas-phase diffusivity for small κ because of the dependence of ζ on the diffusivity.

Rigorous interpretation of flow tube data is hampered by lack of information on the inlet concentration and the inlet concentration distribution, which depends on the injector design. The use of small multiple injectors could provide a more uniform inlet distribution, but the disturbance of the flow field by the injectors cannot be avoided. It is also desirable to adjust the flow rate exiting the injector such that the mean velocity of the injected stream does not differ greatly from the mean velocity of the total flow. That avoids the disruption of the flow field by a high velocity jet exiting the injector.

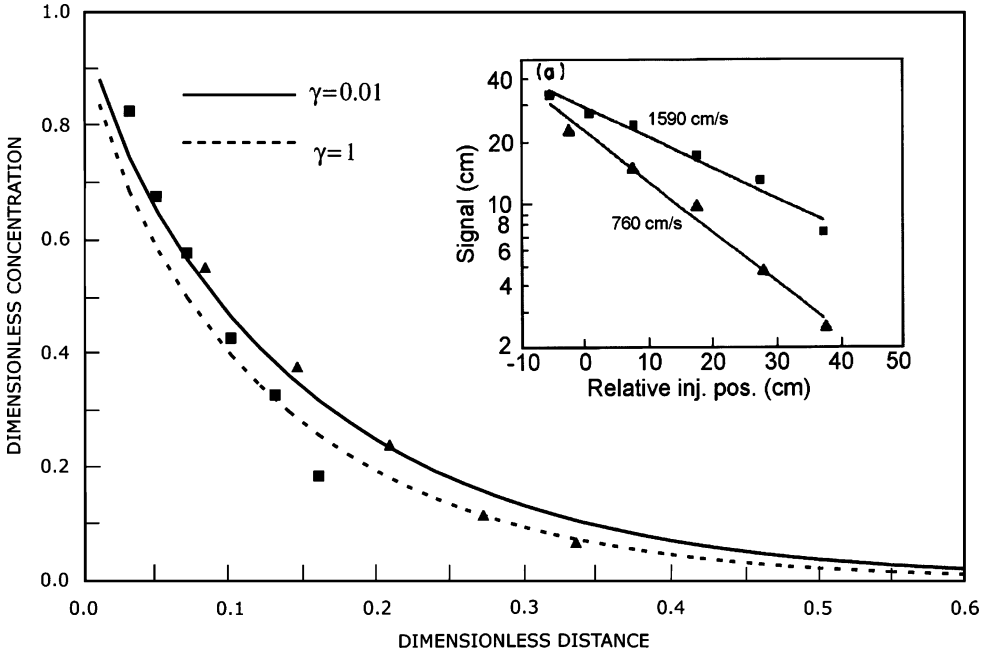

Figure 8. The HO_2/H_2O data of Hanson et al.[3] compared with the wetted-wall tube analysis. The inset is a redrawing of the original graph of the investigators.

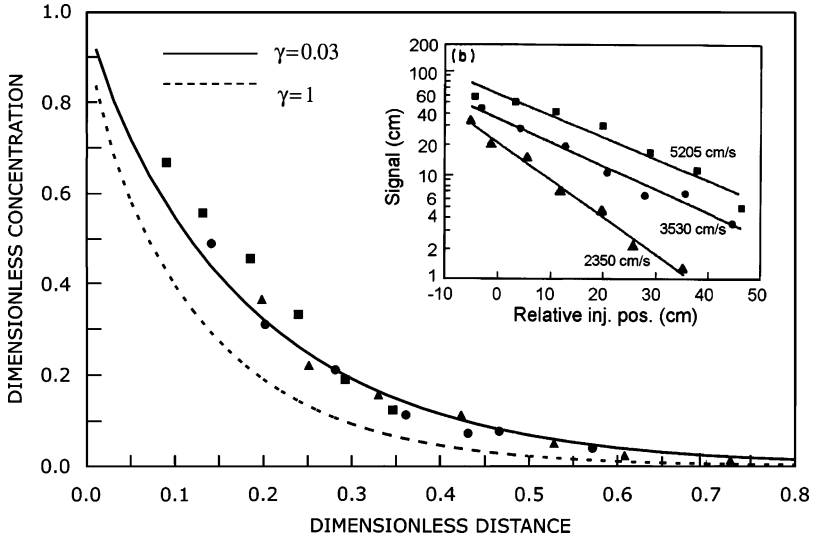

Figure 9. The HO_2/H_2SO_4 data of Hanson et al.[3] compared with the wetted-wall tube analysis. The inset is a redrawing of the original graph of the investigators.

Some comparisons among results for uptake coefficients obtained with wetted-wall columns and those obtained by other methods can be made. For example, the uptake coefficient for O_3 determined from the data of Utter et al. ($\gamma_{O_3} = 0.0008$), which used 0.8 M $Na_2S_2O_3$ as a scavenger, is considerably lower that the uptake coefficients for O_3 reported by Magi et al.[19] using NaI as a scavenger in water. Magi et al. obtained $\gamma_{O_3} = 0.0037-0.0116$ for I^- activities in the range of 0.3615−2.889 at 282 K. However, γ_{O_3} for pure water was found to be too small to be measured by their droplet train technique. Since the Henry's law constant for ozone in water is very low, it is possible that in the Magi experiments, both rapid surface reaction (due preferential concentration of I^- at the interface) and scavenger-assisted uptake occurred, whereas in the Utter experiments, the surface reaction may have been slower.

Thornton and Abbatt[6] reported $\gamma_{HO_2} < 0.01$ for H_2SO_4/H_2O submicrometer aerosol in the absence of Cu(II), but for Cu(II)-doped H_2SO_4, $\gamma_{HO_2} = 0.8 \pm 0.3$. This result is consistent with the uptake coefficients shown in Figure 9 ($0.03 < \gamma_{HO_2} < 1$) based on analysis of the HO_2/H_2SO_4 data of Hanson et al.,[3] but Cooper and Abbatt[5] obtained $\gamma_{HO_2} = 0.025 \pm 0.005$ for H_2SO_4 at 223 K, and Gershenzon et al.[40] reported $\gamma_{HO_2} = 0.2$ for H_2SO_4 at 243 K. The calculations performed for Figures 8 and 9 illustrate that the determination of γ_{HO_2} from wetted-wall tube data is not highly sensitive to the uptake coefficient for $\gamma_{HO_2} > 0.05$.

For OH radicals on a water surface at 293 K, Takami et al.[4] obtained $\gamma_{OH} = 0.0042 \pm 0.0028$ for pH = 5.6, $\gamma_{OH} = 0.0082 \pm 0.0026$ for pH = 1, and $\gamma_{OH} = 0.012 \pm 0.003$ for pH = 11 using an impinging flow method. These uptake coefficients are much lower than the result shown in Figure 6 ($\gamma_{OH} \geq 0.1$) based on the data of Hanson et al.[3] for OH uptake by water, but the effect of ripples on the water film was most likely significant in the wetted-wall column experiments, particularly at higher gas flow rates.

There remains considerable variation in the uptake coefficients for OH on sulfuric acid solutions. Figure 7 indicates that $0.008 \leq \gamma_{OH} \leq 0.04$ based on the wetted-wall data of Hanson and his

co-workers. Baldwin and Golden[51] reported $\gamma_{OH} = 0.00049 \pm 0.00005$ for 96% H_2SO_4 at 298 K using a Knudsen cell, Gershenzon et al.[40] obtained $\gamma_{OH} = 1$ for the same conditions, and Cooper and Abbatt[5] reported $\gamma_{OH} > 0.2$ for 45−96% H_2SO_4 for temperatures in the ranges of 220−230 and 230−298 K. The Knudsen cell technique of Baldwin and Golden involves long time scales during which significant surface saturation effects could arise. Consequently, their results represent a lower limit for γ_{OH}.

The uptake coefficients of OH and HO_2 on sulfuric acid can be expected to vary with the H_2SO_4 concentration because the Henry's law constant and the reactive loss process vary with the water activity.

Acknowledgment. The author thanks the organizers of the Accommodation Coefficient Workshop held at the National University of Ireland, Galway, on April 11 and 12, 2007 for the opportunity to participate in discussions of the state-of-the-art topics related to uptake coefficients and accommodation coefficients of trace gases relevant to atmospheric chemistry. The author is grateful to the reviewers for pointing out that the analysis of transport and chemical reaction in flow tubes applies to a larger class of problems than the determination of uptake coefficients and that the inlet concentration of the reactive gas need not be spatially uniform across the tube cross section.

References and Notes

(1) Kolb, C. E.; Worsnop, D. R.; Zahniser, M. S.; Davidovits, P.; Keyser, L. F.; Leu, M.-T.; Molina, M. J.; Hanson, D. R.; Ravishankara, A. R.; Williams, L. R.; Tolbert, M. A. In *Advances in Physical Chemistry Series*; Barker, J. R., Ed.; World Scientific: Singapore, 1994; Vol. 3.

(2) Davidovits, P.; Kolb, C. E.; Williams, L. R.; Jayne, J. T.; Worsnop, D. R. *Chem. Rev.* **2006**, *106*, 1323−1354.

(3) Hanson, D. R.; Burkholder, J. B.; Howard, C. J.; Ravishankara, A. R. *J. Phys. Chem.* **1992**, *96*, 4979−4985.

(4) Takami, A.; Kato, S.; Shimono, A.; Koda, S. *Chem. Phys.* **1998**, *232*, 215−227.

(5) Cooper, P. L.; Abbatt, J. P. D. *J. Phys. Chem.* **1996**, *100*, 2249−2254.

(6) Thornton, J.; Abbatt, J. P. D. *J. Geophys. Res.* **2005**, *110*, D08309/1−12.

(7) Gershenzon, Y. M.; Grigorieva, V. M.; Ivanov, A. V.; Remorov, R. G. *Faraday Discuss.* **1995**, *100*, 83−100.

(8) Hanson, D. R.; Ravishankara, A. R. *J. Phys. Chem.* **1992**, *96*, 2682−2691.

(9) Robinson, G. N.; Worsnop, D. R.; Jayne, J. T.; Kolb, C. E.; Davidovits, P. *J. Geophys. Res.* **1997**, *102*, 3583−3601.

(10) Hanson, D. R.; Lovejoy, E. R. *Science* **1995**, *267*, 1326−1328.

(11) Hanson, D. R.; Ravishankara, A. R. *J. Geophys. Res.* **1991**, *96*, 17307−17314.

(12) Hanson, D. R.; Ravishankara, A. R. *J. Phys. Chem.* **1993**, *97*, 12309−12319.

(13) Watson, L. R.; Van Doren, J. M.; Davidovits, P.; Worsnop, D. R.; Zahniser, M. S.; Kolb, C. E. *J. Geophys. Res.* **1990**, *95*, 5631−5638.

(14) Shi, Q.; Davidovits, P.; Jayne, J. T.; Worsnop, D. R.; Kolb, C. E. *J. Phys. Chem. A* **1999**, *103*, 8812−8823.

(15) Fried, A.; Henry, B. E.; Calvert, J. G.; Mozurkewich, M. *J. Geophys. Res.* **1994**, *99*, 3517−3532.

(16) Hanson, D. R.; Lovejoy, E. R. *Geophys. Res. Lett.* **1994**, *21*, 2401−2404.

(17) Thornton, J. A.; Braban, C. F.; Abbatt, J. P. D. *Phys. Chem. Chem. Phys.* **2003**, *5*, 4593−4603.

(18) Utter, R. G.; Burkholder, J. B.; Howard, C. J.; Ravishankara, A. R. *J. Phys. Chem.* **1992**, *96*, 4973−4979.

(19) Magi, L.; Schweitzer, F.; Pallares, C.; Cherif, S.; Mirabel, P.; George, C. *J. Phys. Chem. A* **1997**, *101*, 4943−4949.

(20) Gardner, J. A.; Watson, L. R.; Adewuyi, Y. G.; Davidovits, P.; Zahniser, M. S.; Worsnop, D. R.; Kolb, C. E. *J. Geophys. Res.* **1987**, *92*, 10887−10895.

(21) Davis, E. J. *Atmos. Res.* **2006**, *82*, 561−578.

(22) Kaufman, F. *Prog. React. Kinet.* **1961**, *1*, 3−39.

(23) Howard, C. J. *J. Phys. Chem.* **1979**, *83*, 3−9.

(24) Krongelb, S.; Strandberg, M. W. P. *J. Chem. Phys.* **1959**, *31*, 1196−1210.

(25) Poirier, R. V.; Carr, R. C., Jr. *J. Phys. Chem.* **1971**, *75*, 1593−1601.

(26) Judeikis, H. S. *J. Phys. Chem.* **1980**, *84*, 2481−2484.

(27) Donahue, N. M.; Clarke, J. S.; Demerjian, K. L.; Anderson, J. G. *J. Phys. Chem.* **1996**, *100*, 5821−5838.

(28) Graetz, L. *Ann. Phys.* **1885**, *25*, 337−357.

(29) Hsu, C. J. *Appl. Sci. Res.* **1968**, *17*, 359−376.

(30) Gershenzon, Y. M.; Rozenshtein, V. B.; Spasskii, A. I.; Kogan, A. M. *Dokl. Akad. Nauk SSSR* **1972**, *205*, 871−874.

(31) Abramowitz, M.; Stegun, I. A. *Handbook of Mathematical Functions*; National Bureau of Standards Applied Mathematics Series 55; U.S. Government Printing Office: Washington, 1964.

(32) Nicolaon, G.; Cooke, D. D.; Davis, E. J.; Kerker, M.; Matijevic, E. *J. Colloid Interface Sci.* **1971**, *35*, 490−501.

(33) Davis, E. J.; Nicolaon, G. *J. Colloid Interface Sci.* **1971**, *37*, 768−778.

(34) Gershenzon, Y. M.; Rozenshtein, V. B.; Spasskii, A. I.; Kogan, A. M. *Dokl. Akad. Nauk SSSR* **1972**, *205*, 624−627.

(35) Orkin, V. L.; Khamaganov, V. G.; Larin, I. K. *Int. J. Chem. Kinet.* **1993**, *25*, 67−78.

(36) Brown, R. L. *J. Res. Natl. Bur. Stand.* **1978**, *83*, 1−8.

(37) Walker, R. E. *Phys. Fluids* **1961**, *4*, 1211−1216.

(38) Segatz, J.; Rannacher, R.; Wichmann, J.; Orlemann, C.; Dreier, T.; Wolfrum, J. *J. Phys. Chem.* **1996**, *100*, 9323−9333.

(39) Davis, E. J. *Can. J. Chem. Eng.* **1973**, *51*, 562−572.

(40) Gershenzon, Y. M.; Ivanov, A. V.; Kucheryavii, S. I.; Rozenshtein, V. B. *Kinet. Katal.* **1986**, *27*, 928−932.

(41) Aubin, D. G.; Abbatt, J. P. D. *J. Phys. Chem. A* **2007**, *111*, 6263−6273.

(42) Bird, R. B.; Stewart, E. N.; Lightfoot, E. N. *Transport Phenomena*, 2nd ed.; Wiley: New York, 2002.

(43) Khalizov, A. F.; Earle, M. E.; Johnson, W. J. W.; Stubley, G. D.; Sloan, J. J. *J. Aerosol Sci.* **2006**, *37*, 1174−1187.

(44) Khalizov, A. F.; Earle, M. E.; Johnson, W. J. W.; Stubley, G. D.; Sloan, J. J. *Rev. Sci. Instrum.* **2006**, *77*, 033102-1−033102-9.

(45) Papoutsakis, E.; Ramkrishna, D.; Lim, H. C. *Appl. Sci. Res.* **1980**, *36*, 13−34.

(46) Papoutsakis, E.; Ramkrishna, D.; Lim, H. C. *AIChE J.* **1980**, *26*, 779−787.

(47) Acrivos, A. *Appl. Sci. Res.* **1980**, *36*, 35−40.

(48) Davis, E. J.; Bonano, E. J. *Chem. Eng. Sci.* **1979**, *34*, 439−440.

(49) Boucher, D. F.; Alves, G. E. *Chem. Eng. Prog.* **1959**, *55*, 55−64.

(50) Boucher, D. F.; Alves, G. E. *Chem. Eng. Prog.* **1963**, *59*, 75−83.

(51) Baldwin, A. C; Golden, D. M. *J. Geophys. Res.* **1980**, *85*, 2888−2889.